JOINT EUROPEAN TORUS

JET–P(90)13

F. Pegoraro, F. Porcelliand T.J. Schep

Large Gyroradius m = l Alfven Modes and Energetic Particles

Large Gyroradius m = 1 Alfven Modes and Energetic Particles

F. Pegoraro, F. Porcelli, T.J. Schep and JET Team*

JET-Joint Undertaking, Culham Science Centre, OX14 3DB, Abingdon, UK

** See Appendix 1*

Preprint of Paper to be submitted for publication in
Physics of Fluids B

ABSTRACT.

Non-magnetohydrodynamic effects, caused by a minority population of energetic particles and/ or by the large gyroradii of the main ion population, strongly modify the stability of a high temperature toroidal plasma against m = 1 internal modes. We show that the enhanced stability due to the presence of the energetic particles is reduced in the large gyroradius regime, where the width of the transition layer of the mode is determined by the gyroradius of main ions. This modification results from the presence of a discrete spectrum of resistively damped Alfven-type modes which can be destabilised through the resonance with the energetic ions.

I INTRODUCTION

The repetitive temperature relaxations of the central part of the plasma column in a toroidal configuration (sawtooth oscillations) pose a potential threat to the achievement of ignition conditions. On the other hand, a minority population of energetic ions, produced for example by auxiliary heating at the ion-cyclotron frequency, has been experimentally recognised [1] and theoretically demonstrated [2-6] to improve the plasma stability against these relaxations, leading in the JET experiment to periods, long on the energy confinement timescale, during which sawteeth are absent. The same stabilisation mechanism has also been predicted [3,7] to apply to the naturally occurring α-particles in an ignited Deuterium-Tritium (D-T) plasma. Indeed, α-particles can extend the stable value of the plasma poloidal beta parameter β_p as much as three to four times above its value as determined within the ideal magnetohydrodynamic (MHD) approximation. This prediction has made the experimental JET findings of sawtooth suppressed regimes directly relevant to the identification of the ignition regimes that are achievable as far as global MHD stability is concerned.

It has been indicated [7] that for the high temperature and relatively large β_p values that are expected in an igniting plasma, the relevant stability condition is determined by the branch of the m = 1 internal modes that is related to the excitation of the so-called "fishbone" oscillations. These oscillations, first detected in the Poloidal Divertor Experiment in Princeton [8] and subsequently in other experimental devices including JET [9], are interpreted [10-12] as arising from the resonant, i.e. dissipative, response of the energetic ions, whereas the reactive part is responsible for the enhanced stability when the mode frequency is small compared with the characteristic magnetic drift frequency of the energetic ions, ω_{Dh}. Indeed, sawtooth stabilisation and fishbone excitation have been shown [3,7] to be directly related phenomena. Inside the stability domain both sawteeth and fishbone oscillations are stable. The stability domain in the $\hat{\gamma}_{mhd} - \hat{\beta}_{ph}$ plane is given in Fig. 6

or Ref. 7. In that figure $\hat{\gamma}_{mhd} \equiv \gamma_{mhd} / \omega_{Dh}$ is the normalised MHD growth rate which increases with the poloidal beta parameter, β_p, of the bulk plasma, and $\hat{\beta}_{ph}$ is a suitably normalised poloidal beta of the energetic particles (see Eq. (23) below). Fishbone oscillations turn unstable in a parameter "band" boundarying the stability domain at larger values of β_p and/or of $\hat{\beta}_{ph}$. Further away from this band, the instability turns from resonantly driven to fluid-like and takes the characteristics of an ideal MHD internal mode driven by both the pressure gradient of the bulk plasma and of the energetic ions. Along the marginal stability curve that defines the stable domain, the mode frequency increases from ω_{di} at small $\hat{\beta}_{ph}$, to ω_{Dh} at larger $\hat{\beta}_{ph}$, where ω_{di} is the bulk ion diamagnetic frequency evaluated at the mode transition layer (i.e. at $r = r_o$ with $q(r_o) = 1$, r the radial coordinate and q the magnetic winding number). This frequency excursion includes the two frequency regimes that were considered in Ref. 10 and in Ref. 11, respectively, in order to interpret the observed fishbone oscillations. These two regimes merge and the stable domain disappears if $\omega_{di} \sim \omega_{Dh}$, which was the regime relevant to the PDX experiments [8].

The above analysis has been mainly developed for plasma conditions such that the mean gyroradius of the bulk ions is smaller than the width of the mode transition layer at $r = r_o$. However, this condition may not be satisfied in a high temperature igniting plasma. We recall that within the fluid theory the width of this layer is determined either by ion inertia or by electron resistivity. On the other hand it is determined by the size of the ion gyroradius ρ_i when this becomes large. A detailed investigation of internal modes in this "ion kinetic regime" has been presented in Ref. 13 based on the analysis of resistive modes in the so-called semi-collisional regime [14].

In the present paper we extend the results of Ref. 13 by including the effect of an energetic ion population with a magnetic precession frequency ω_{Dh} which is much larger than the bulk ion diamagnetic frequency ω_{di} as is the case in an ignited plasma. Our aim is to determine the stability domain obtained when the large size

of the bulk ion gyroradii is taken into account and to compare it to the results of fluid theory [7,15]. Similar results have been obtained numerically using an improved model for the electrical resistivity, valid in the low collisionality limit [16].

We find that for large values of $(\rho_i/r_o\varepsilon_\eta^{1/3})$, where $\rho_i = c(T_i m_i)^{1/2}/eB$, and ε_η is the inverse magnetic Reynolds number, the parameter domain where low frequency ($\omega \sim \omega_{di}$) resonant (fishbone) modes occur is enlarged. This decrease of the stable domain occurs at lower values of $\hat{\beta}_{ph}$. Fishbone modes can in principle occur for values of the bulk plasma poloidal beta β_p below the ideal MHD threshold, in contrast to the results of fluid theory. However, for values of $(\rho_i/r_o\varepsilon_\eta^{1/3})$ that are relevant to ignition regimes, the extension of the fishbone domain is smaller. For larger values of β_{ph}, corresponding to oscillations with frequency $\omega \sim \omega_{Dh}$, the fluid result is essentially recovered as long as the condition $\rho_i/r_o << \omega_{Dh}/\omega_A$ is met.

Physically, the reduction of the stability domain results from the presence in the large ion gyroradius regime of a discrete spectrum of resistively damped Alfvén-type modes which, for vanishing $\varepsilon_\eta^{1/3}r_o/\rho_i$, accumulate at a limiting frequency ω_ρ, defined in Eq. (10) below. Both their frequency and damping rate have inverse logarithmic dependences on $\varepsilon_\eta^{1/3}r_o/\rho_i$. The energetic ions can resonately destabilise the modes in the lower frequency portion of the spectrum. As the parameter $\varepsilon_\eta^{1/3}r_o/\rho_i$ is increased, the number and the growth rate of the unstable modes decrease.

The appearance of a resistive correction in logarithmic form is related to the asymptotic behaviour of the mode amplitude when the layer where resistivity is important is approached. In this layer the two independent solutions of the dispersion equation behave as powers of the independent variable (see Eq. (B6) of Ref. [13]). For modes with real frequency $\omega \sim \omega_\rho$, the exponents become complex conjugate so that a dissipative mechanism in Ohm's law (for example resistivity or electron viscosity) must be invoked in order to regularise the amplitudes. As a

consequence, the small parameter associated with this mechanism enters the dispersion relation through a logarithmic term.

II DISPERSION RELATION

We refer to the results of Refs. 13 and 14 where the mode dispersion relation is obtained as follows. Inside the transition layer non-ideal effects like resistivity and parallel compressibility are taken into account in the electron response. The ion response is calculated to all orders in the ion gyroradius. The width of the layer is determined by the ion gyroradius, while resistivity is important in a narrow sub-layer. These responses are treated in a Fourier space representation. In this representation the Fourier variable is interpreted as the radial wave vector. In a plasma configuration with finite shear at the q = 1 surface, the plasma contribution from the ideal MHD region outside the layer takes the form of a boundary condition to be imposed at small values of the Fourier variable. This boundary condition depends on a single parameter which is denoted by λ_H (first introduced in Ref. 17), and which is proportional to the negative of the energy functional δW. The resulting dispersion equation is solved in Fourier space by a double asymptotic matching procedure. A simplification is achieved by adopting an approximation of the full ion kinetic response [14] that bridges the small gyroradius limit (corresponding to small values of the radial wave number variable) to the large gyroradius limit (corresponding to large radial wave numbers). This approximation is applicable to modes for which the effect of the gradient of the ion temperature T_i is not crucial as is the case for modes with $\omega < \omega_{di}$ [13]. In the following we shall take $d\ell nT_i / d\ell nn = 0$.

The energetic ion population modifies the plasma response outside the boundary layer and, as discussed in detail in Ref. 7 (see also references therein), can be accounted for by the substitution

$$\lambda_H \rightarrow \lambda_{HK} \equiv \lambda_H + \lambda_K(\omega). \tag{1}$$

For an isotropic distribution the complex function $\lambda_K(\omega)$ can be written as

$$\lambda_K(\omega) = \left(\varepsilon_o^{3/2}\beta_{ph} / s_o\right)\Lambda_K(\omega), \tag{2}$$

where $\varepsilon_o = r_o/R_o$, $s_o = r_o(dq/dr)_{r_o}$,

$$\beta_{ph} = \frac{-8\pi}{B_p^2(r_o)}\int_0^1 dx\, x^{3/2} dp_h / dx, \tag{3}$$

p_h is the hot particle pressure and $\Lambda_K(\omega)$ is a frequency dependent form factor.

The real part of $\Lambda_K(\omega)$ represents the reactive response of the energetic ions and is negative (stabilising) for lower frequencies and positive for higher frequencies. The imaginary part of $\Lambda_K(\omega)$ represents the velocity dependent resonant interaction with the precessing energetic ions and is negative for $\omega/\omega_{Dh} > 0$. A plot of $\Lambda_K(\omega)$ for real ω is shown for a slowing down, isotropic α-particle distribution function in Fig. 1, where $\omega_{Dh} = c\varepsilon_h/(eBR_or_o)$ is the orbit averaged precession frequency of deeply trapped α-particles with birth energy $\varepsilon_h = 3.5$ MeV in a D-T plasma, evaluated at $r = r_o$.

The resulting dispersion relation can be written in the form [13, 14]

$$\frac{L(\lambda_{HK},\omega) + iF(-\nu)}{L(\lambda_{HK},\omega) + iF(\nu)} = \frac{H(\nu)}{H(-\nu)}(i/\varepsilon)^{\nu}. \tag{4}$$

Here,

$$L(\lambda_{HK},\omega) = \frac{\omega_A[\lambda_H + \lambda_K(\omega)]}{[\omega(\omega-\omega_{di})]^{1/2}}, \tag{5}$$

with $\omega_A = V_A/(R_o\sqrt{3})$, $V_A = (B^2/4\pi\rho_m)^{1/2}$, ρ_m the mass density, R_o the torus major radius, and $\omega_{di} = -[(c/eBrn)(dp_i/dr)]_{r_o}$. The function F(ν) is defined by

$$iF(\nu) = 8\left(\tfrac{1}{4}-\nu^2\right)^{-3/2}\Gamma^2\left(\tfrac{5}{4}+\tfrac{1}{2}\nu\right)/\Gamma^2\left(-\tfrac{1}{4}+\tfrac{1}{2}\nu\right), \tag{6}$$

with

$$\nu^2 = \tfrac{1}{4} - \frac{(\omega-\omega_{*e})(\omega-\omega_{di})}{(1+\tau)(\rho_i/r_o)^2 s_o^2\omega_A^2}, \tag{7}$$

ω_{*e} being the electron drift mode frequency and $\tau = T_e/T_i$ the ratio of the electron and ion temperatures. In the right hand side of Eq. (4),

$$H(\nu)=2^{\nu}\Gamma^2(\nu)\,\Gamma^2\left(\tfrac{5}{4}-\tfrac{1}{2}\nu\right), \tag{8}$$

and

$$\varepsilon=\varepsilon_\eta\frac{(\omega-\omega_{*e})(\omega-\omega_{di})}{\omega s_o^4\omega_A(1+\tau)^2(\rho_1/r_o)^4}, \tag{9}$$

with $\varepsilon_\eta = \eta_{\parallel}s_o^2c^2/(4\pi r_o^2\omega_A)$ the inverse magnetic Reynolds' number, and $\eta_{\parallel}$ the parallel resistivity. In the semi-collisional regime under consideration, $|\varepsilon| << 1$. In the derivation of Eq. (4) an isothermal equation of state has been assumed for the electrons. Moreover, since the ion temperature gradient has been neglected, $\omega_{*e} = -\omega_{di}/\tau$. For the sake of simplicity we shall take $\tau = 1$ and ω_{di} positive. Since Eq. (4) is symmetrical for $\nu \to -\nu$, a convenient prescription can be adopted in defining ν from (7). We choose Im $\nu \le 0$, which corresponds in the case of growing ion modes to Re $\nu > 0$.

For ion modes with real frequencies in the range $\omega_{di} \le \omega \le \omega_\rho$, we have $0 \le \nu \le 1/2$, where ω_ρ is defined by $\nu(\omega = \omega_\rho) = 0$,

$$\omega_\rho^2=\omega_{di}^2+\tfrac{1}{2}\left(\frac{\rho_i}{r_o}\right)^2 s_o^2\omega_A^2 . \tag{10}$$

In this frequency range $F(\nu)$ is purely imaginary. For larger real frequencies, ν becomes imaginary and $F(\nu)$ is complex, while for purely growing modes, $\nu^2 > 1/4$ and $F(\nu)$ is real. In the limit of large frequencies, $|\nu| \to \infty$, and $F(\nu) \to 1$. A plot of Re $F(\nu)$ and Im $F(\nu)$ is shown in Fig. 2.

Before focussing our attention on marginally stable modes with frequency $\omega > \omega_{di}$, corresponding to $-\infty < \nu^2 < 1/4$, it is useful to discuss first the general properties of the dispersion relation (4), by considering the frequency behaviour of its right hand side. If the r.h.s. is large, the leading order dispersion equation according to (4) is [7]

$$L(\lambda_{HK},\omega)=-iF(\nu). \tag{11}$$

Due to the smallness of ε, this dispersion equation is obtained for finite and positive values of Re ν, i.e. for growing modes. For Re ν finite and negative, i.e. for damped modes, the r.h.s. of Eq. (4) is small, and Eq. (11) with $\nu \to -\nu$ is obtained. On these

modes resistivity leads to corrections proportional to powers of ε_η, except when $\nu \cong 1/2$, in which case, Eq. (6) yields $F(\nu) \to 0$. In the latter limit resistivity plays an essential role leading to semi-collisional tearing and m = 1 internal modes as discussed in Refs. [13] and [14]. For real positive values of ν in the range $\nu < 1/2$ and not too close to zero, marginally stable modes can be found in the range $\omega_{di} < \omega < \omega_\rho$ if λ_{HK} is real and larger than the negative value

$$\lambda_{H\,\min} = -2\sqrt{2}\left[\Gamma^2(1/4)/\Gamma^2(-1/4)\right]\left[\omega_\rho/\left(\omega_\rho+\omega_{di}\right)\right]^{1/2}(\rho_i/r_0). \tag{12}$$

These modes are destabilised by the resonant interaction with the energetic ions, i.e. by Im λ_K. Thus, Eq. (12) represents the extension of the low frequency fishbone domain to negative values of λ_H, i.e. to values of β_p below the ideal MHD threshold. However this result is only indicative since, as will be illustrated later in this section, the effect of resistivity cannot be neglected as ν approaches zero.

Next we consider the high frequency limit in which $\nu \propto -i\omega$. The asymptotic behaviour of the r.h.s. of Eq. (4) is

$$\frac{H(\nu)}{H(-\nu)}(i/\varepsilon)^\nu \propto \exp\left[\nu\left(-2+2\ell n 4|\nu|+2i\arg\nu - i\,\pi\sigma + i\pi/2 - \ell n\,\varepsilon\right)\right], \tag{13}$$

where σ = sign (arg ν). Expression (13) is a fast oscillating function of the frequency. Its amplitude is finite for modes with almost real frequencies (arg $\nu \cong -\pi/2$, $\sigma = \pm 1$) such that

$$\mathrm{Re}\left[\ell n\left(16|\nu|^2/\varepsilon\right)+i\nu\pi/2\right] = 0(1). \tag{14}$$

This balance corresponds to the high frequency Alfvén-type modes (see Eq. (63) in Ref. [14]). Their dispersion relation is mainly governed by the fast oscillating exponential. For this reason the MHD boundary conditions play a minor role on these modes. As shown by Eq. (14), these modes are weakly damped with

$$\frac{\mathrm{Im}\,\omega}{\mathrm{Re}\,\omega} \cong -\frac{\pi/2}{\ell n\left(16|\nu|^2/\varepsilon\right)}. \tag{15}$$

If this balance is not satisfied, i.e. for larger damping or growth rates and for purely oscillatory modes, the dispersion relation (11) is recovered with $F(\nu) \to 1$. If all resistive corrections are disregarded, this dispersion relation is identical to that of internal m = 1 fluid modes. The ideal MHD growth rate, $\gamma = \gamma_{MHD} \equiv \lambda_H \omega_A$, is obtained from (11) in the limit $\omega_\rho / \gamma_{mhd} \to 0$ and no energetic particles ($\lambda_K = 0$).

Modes similar to the high-frequency Alfvén-type modes are also found for intermediate values of ν close to the imaginary axis and for small values of ν. For these values $H(\nu)/H(-\nu)$ is a finite quantity so that the magnitude of the r.h.s. of (4) is determined by the factor $(i/\varepsilon)^\nu$ which is finite for

$$\mathrm{Re}\left(\nu \ell n\, \varepsilon\right) \cong 0(1). \tag{16}$$

The mhd boundary conditions play an increasingly important role for decreasing ν because the r.h.s. of Eq. (4) oscillates more slowly and all contributions to the dispersion relation become of the same order of magnitude. As will be shown shortly, modes in this range of values of ν are resistively damped in the absence of energetic particles, i.e. for real boundary conditions λ_{HK}. The resonant interaction with the energetic ions tends to destabilise these modes.

We are interested in marginal stability for modes with frequency $\omega > \omega_{di}$. Near ω_{di}, ν is real and positive and the dispersion relation (11) is valid, as discussed above. When ω approaches ω_ρ, $\nu \to 0$ and the full dispersion relation has to be considered. For larger frequencies, ν is negative imaginary, and for sufficiently large frequencies the dispersion relation (11) is again recovered.

To treat analytically modes with frequencies around ω_ρ we consider the ordering

$$\nu\, \ell n\, 1/\varepsilon = 0(1). \tag{17}$$

With this ordering the dispersion relation (4) becomes

$$\frac{L\left(\lambda_{HK}, \omega_\rho\right) + iF(0) - i\nu\, F'(0)}{L\left(\lambda_{HK}, \omega_\rho\right) + iF(0) + i\nu\, F'(0)} = (1 + i\alpha\nu)\exp\left[\nu\, \ell n(1/\varepsilon)\right], \tag{18}$$

where ε is evaluated at $\omega = \omega_\rho$, $F(0) = -4i\,\Gamma^2(1/4)/\Gamma^2(-1/4)$, $F'(0) = F(0)[\psi(5/4) - \psi(-1/4)]$ with $\psi(z) = \Gamma'(z)/\Gamma(z)$ and

$$\alpha = (\pi/2) - 2i\left[\ell n 2 + \psi(1) - \psi(5/4)\right]. \tag{19}$$

The imaginary contribution to α arises from the expansion of $H(\nu)/H(-\nu)$. In terms of the normalised variables

$$x = \left[\left(L\left(\lambda_{HK}, \omega_\rho\right) + iF(0)\right)/iF'(0)\right]\ell n(1/\varepsilon),$$
$$\bar{\nu} = \nu\,\ell n(1/\varepsilon) \qquad \text{and} \qquad \bar{\alpha} = \alpha/\ell n(1/\varepsilon) << 1, \tag{20}$$

Eq. (18) can be written as

$$x = -\bar{\nu}\,ctgh\left[\bar{\nu}/2\left(1 + i\bar{\alpha}\right)\right]. \tag{21}$$

The small ν limit of Eq. (11) is recovered from (21) for Re $\bar{\nu} >> 1$, where Eq. (16) is violated. In the absence of energetic ions $L(\lambda_{HK},\omega_\rho)$ is real. To leading order in $(\ell n\ 1/\varepsilon)^{-1}$, Eq. (21) gives, for fixed x, $-\infty < x < +\infty$, a discrete spectrum of undamped modes with frequencies Re $\omega = \omega_\rho + O[(\ell n\ 1/\varepsilon)^{-3}]$ that accumulate at $\omega = \omega_\rho$. The damping rate, Im ω - $O[(\ell n\ 1/\varepsilon)^{-3}]$, is obtained by including the first order quantity α.

This spectrum of damped modes is destabilised by the resonant interaction with the energetic ions. The resulting marginal stability curve is obtained by solving (21) for x as a function of imaginary t ($\omega > \omega_\rho$). According to Eq. (21), the imaginary part of $\bar{\alpha}$ can be removed by rescaling x and t. Taking $\bar{\alpha}$ to be real, Eq. (21) can be rewritten in the form

$$\left[\mathrm{Im}\,x - \frac{1 + i\bar{\alpha}t}{\bar{\alpha}}\right]^2 + (\mathrm{Re}\,x)^2 = \frac{1 + \frac{1}{3}\bar{\alpha}^2 t^2}{\bar{\alpha}}, \tag{22}$$

which is a spiral curve in the complex x-plane. Since $t^2\bar{\alpha}^2$ becomes increasingly negative and $it\bar{\alpha}$ increasingly positive with increasing frequency, the radius of the spiral decreases and its "instantaneous" centre moves along the imaginary axis away from the point Im $x = \bar{\alpha}^{-1}$. This radius is very large on the normalised x scale due to modes with $\bar{\nu} \cong -i\pi$. This implies that along the marginal stability curve Re λ_{HK} and Im λ_{HK} undergo excursions that are of order one and are independent of resistivity to leading order in $1/\ell n(1/\varepsilon)$. Thus the relevant zero resistivity limit is obtained by first setting the mode growth rate equal to zero and by taking

subsequently the limit of vanishing resistivity. Note that since the resistivity enters logarithmically in the dispersion relation, the theoretical limit of zero resistivity involves values of ε that are unrealistic.

For realistic values of the magnetic Reynolds number, $\ell n(1/\varepsilon)$ is large but still finite so that the dispersion relation (4) has to be solved numerically. We limit ourselves to modes with frequency $\omega \gtrsim \omega_\rho$. In Fig. 3, the marginal stability curve is shown in the complex λ_{HK} plane for $\omega_{di}/\omega_{Dh} = 0.07$, $\omega_\rho/\omega_{Dh} = 0.12$ and $\omega_\rho/(\omega_A \varepsilon_\eta^{1/3}) = 8.5$, corresponding to $\varepsilon(\omega = \omega_\rho) \cong 1.5 \times 10^{-4}$. Since $\ell n(1/\varepsilon)$ is finite, the number of times the spiral winds upon itself is limited and its centre shifts with the frequency along the imaginary λ_{HK} axis. At larger frequencies the oscillations disappear and the curve corresponds to that obtained in the limit of Eq. (11). In Fig. 4, the real and imaginary parts of λ_{HK} are given as a function of $|v|$ for the same values of the relevant parameters as in in Fig. 3. For small $|v|$, the curves in Fig. 4 are reminescent of the functional behaviour in Eq. (21). The marginal stability curve of Fig. 3 translates into the solid curve of Fig. 5 in the $\left(\hat{\gamma}_{mhd}, \hat{\beta}_{ph}\right)$ plane, where

$$\hat{\beta}_{ph} \equiv (\varepsilon_o \beta_{ph}/S_o)(\omega_A/\omega_{Dh}). \tag{23}$$

This curve is interrupted for ω approaching ω_{di}. The stable domain lies below and to the left of this line. Inside the spiral structure more than one mode can be unstable with Re $\omega \approx \omega_\rho$, while elsewhere only one mode with $\omega_{Dh} \gtrsim$ Re $\omega > \omega_\rho$ is unstable. The right boundary of the stable domain corresponds to large negative values of v^2 ($\omega \sim \omega_{Dh}$) and therefore depend very weakly on resistivity. On the other hand, the left boundary at low values of $\hat{\beta}_{ph}$ (missing in Fig. 5) requires an analysis of modes with Re $\omega < \omega_{di}$. This frequency range has been studied with the two fluid model for the plasma bulk [4] and leads to the threshold indicated by the part of the dashed line adjoining $\hat{\beta}_{ph} = 0$ in Fig. 5. The latter line intercepts a second dashed curve corresponding to the two-fluid marginal stability at higher frequency ($\omega > \omega_{di}$). We expect a similar stability boundary for Re $\omega < \omega_{di}$ in the core-ion kinetic regime. In fact, in this regime, similarly to the two-fluid case, growth rates

scale as a linear power of resistivity at sufficiently large diamagnetic frequencies [ω_{di}, $\omega_{*e} > (\rho_i/r_o\varepsilon_\eta^{1/3})^{-4/7}\omega_A$] and in the absence of energetic ions [13]. For comparison, the marginal stability solution of Eq. (11), which is obtained when the limit $\ell n(1/\varepsilon) \rightarrow \infty$ is taken before the limit $\gamma/\omega_\rho = \rightarrow 0$, is represented by the dotted curve of Fig. 5 for the same values of ω_{di}/ω_{Dh} and ω_ρ/ω_{Dh}.

As resistivity is decreased, the ascending part of the stability boundary shifts towards negative values of $\hat{\gamma}_{mhd}$, so that the stable domain becomes narrower, while the region interested by the spiral structure increases until a limiting area is approached as $\ell n(1/\varepsilon) \rightarrow \infty$. The mathematical limit of zero resistivity, taken after the growth rate has been set to zero, is illustrated by the dashed curve of Fig. 6. The marginal stability condition now yields a spiral structure which fills densely the limiting region enclosed by the dashed curve. In this region, an infinite number of roots are degenerate at marginal stability with a frequency $\omega = \omega_\rho$. The solid line corresponds to $\gamma/\omega_\rho = 10^{-3}$ and $\omega_\rho/(\omega_A\varepsilon_\eta^{1/3}) = 85$, yielding $\varepsilon(\omega_\rho) \cong 1.5 \times 10^{-7}$. The latter value is rather extreme and is shown here for the purpose of illustration. In this case, many roots with Re $\omega \approx \omega_\rho$ are unstable within the spiral structure.

III CONCLUSIONS

We have investigated the linear stability of m = 1 modes in a magnetically confined plasma in the presence of energetic particles, taking into account the full gyroradius effects of the thermal ions as well as the effects of a small but finite electrical resistivity. Assuming, for simplicity, equal thermal electron and ion temperatures and neglecting the thermal ion temperature gradient, the stability condition depends on five normalised parameters, which can be chosen as:

(i) the ideal MHD energy functional, $\hat{\gamma}_{mhd} \equiv \lambda_H\omega_A/\omega_{Dh}$;

(ii) the poloidal beta of the energetic ions, $\hat{\beta}_{ph} \equiv (\varepsilon_o\beta_{ph}/s_o)(\omega_A/\omega_{Dh})$;

(iii) the ion diamagnetic frequency, ω_{di}/ω_{Dh};

(iv) the ion Larmor radius, $\hat{\rho}_i = (s_o\rho_i/r_o)(\omega_A/\omega_{Dh})$;

(v) and the reciprocal Reynolds number, ε_η.

We have focussed our attention on modes which oscillate with a frequency of the order of, or larger than the ion diamagnetic frequency. At the highest values of the bulk β_p, i.e. for larger and positive λ_H, these modes are essentially ideal MHD internal kinks, largely unaffected by the non-ideal effects. As discussed, e.g. in Ref. [7], if $\omega_{di} << \omega_{Dh}$, the ideal MHD stability threshold is raised in the presence of energetic ions from $\lambda_H = 0$ to a positive value which increases linearly with β_{ph}, i.e. $\lambda_H \sim \varepsilon_o \beta_{ph}/s_o$, up to a maximum value corresponding to $\hat{\gamma}_{mhd} \sim 0.5$. Near the marginal stability curve, modes with $\omega_{di} \lesssim \mathrm{Re}\,\omega \lesssim \omega_{Dh}$ tend to be damped by resistivity, but are destabilised by the resonant interaction with the fast ions, giving rise to fishbone-like oscillation bursts.

The interesting feature of the large ion gyroradius regime is that a new frequency, $\omega_\rho = [\omega_{di}^2 + (\rho_i/2r_o)^2 s_o^2 \omega_A^2/2]^{1/2}$, is introduced. For small ω_{di}, this frequency corresponds to the Alfvén frequency $k_{||} V_A \sim s_o x V_A/R$, where $r_o x \equiv (r - r_o)$ is of the order of the width of the transition layer, $\delta \sim \rho_i/\sqrt{2}$. We have shown that these modes exist as localised modes in the presence of resistivity even for negative values of λ_H. In principle, this could allow the excitation of low frequency fishbone modes for values of β_p below the ideal MHD threshold, as pointed out in Ref. 7. However, the resistive damping becomes quite strong in this case and, being proportional to $(\ell n\, \varepsilon_\eta)^{-1}$, weakly dependent on the value of the magnetic Reynolds number, so that for realistic parameters the unstable fishbone region at negative λ_H is practically wiped out. Nonetheless, the new frequency ω_ρ guarantees the existence of a low frequency fishbone regime even when ω_{di} is negligible.

For values of $\hat{\rho} << 1$, the high frequency portion of the marginal stability curve, near which high frequency fishbones with $\omega \sim \omega_{Dh}$ are expected to be excited, is not significantly modified.

In a D-T ignition experiment, where alpha particles with an energy $\varepsilon_\alpha \sim 3.5$ MeV are produced, typically one has $\omega_{di}/\omega_{Dh} << 1$ and $\hat{\rho} \sim 0.1$. For these

parameters, the erosion of the left boundary of the stable domain by an amount $\Delta\beta_{p\alpha} \sim (s_o/\varepsilon_o^{3/2})(\rho_i/r_o)$ as discussed in Ref. [7], is partly compensated by the resistive damping, while the maximum value of β_p that can be stabilised in the presence of the alpha particles remains largely unaffected.

Acknowledgement

Discussions with H.L. Berk and Y.Z. Zhang are gratefully acknowledged. This work was performed in part within the Association agreement between Euratom and FOM with financial support from N.W.O. Financial support from the Scuola Normale Superiore is also acknowledged.

References

[1] D. Campbell, et al., in Proceedings of the 15th European Conference on Controlled Fusion and Plasma Physics, Dubrovnik (EPS, Petit-Lancy, Switzerland 1988), Vol. 12B, Part I, 377.

[2] B. Coppi, R.J. Hastie, S. Migliuolo, F. Pegoraro and F. Porcelli, Phys. Lett. A, 132, 267 (1988).

[3] F. Pegoraro, F. Porcelli, B. Coppi, P. Detragiache and S. Migliuolo, in Plasma Physics and Controlled Nuclear Fusion Research 1988, Proceedings of the 12th International Conference, Nice (International Atomic Energy Agency, Vienna, 1989), Vol. II, p.243.

[4] B. Coppi, P. Detragiache, S. Migliuolo, F. Pegoraro and F. Porcelli, Phys. Rev. Lett. 63, 2733 (1989).

[5] R.B. White, P.H. Rutherford, P. Colestock and M.N. Bussac, Phys. Rev. Lett. 60, 2038 (1988).

[6] R.B. White, M.N. Bussac, F. Romanelli, Phys. Rev. Lett. 62, 539 (1989).

[7] B. Coppi, S. Migliuolo, F. Pegoraro and F. Porcelli, Phys. Fluids, in press.

[8] G. McGuire, R. Goldston, M. Bell, M. Bitter, K. Bol, K. Brau, D. Buchenauer, T. Crowley, S. Davis, F. Dylla, H. Eubank, H. Fishman, R. Fonck, B. Grek, R. Grimm, R. Hawryluk, H. Hsuan, R. Huse, R. Izzo,R. Kaita, S. Kaye, H. Kugel, D. Johnson, J. Manickam, D. Manos, D. Mansfield, E. Mazzucato, R. McCann, D. McCune, D. Monticello, R. Motley, D. Mueller, K. Oasa, M. Okabayashi, K. Owens, W. Park, M. Reusch, N. Sauthoff, G. Schmidt, S. Sesnic, J. Strachan, C.

Surko, R. Slusher, H. Takahashi, F. Tenney, P. Thomas, H. Towner, J. Valley and R. White, Phys. Rev. Lett. 50, 891 (1983).

[9] M.F.F. Nave, E. Joffrin, F. Pegoraro, F. Porcelli, P. Smeulders and K. Thomsen, in Proceedings of the 16th European Conference on Controlled Fusion and Plasma Heating, Venice (EPS, Petit-Lancy, Sqitzerland, 1989), Vol. 13B, Part II, 505.

[10] B. Coppi and F. Porcelli, Phys. Rev. Lett. 57, 2272 (1986).

[11] L. Chen, R.B. White and M.N. Rosenbluth, Phys. Rev. Lett. 52, 1122 (1984).

[12] B. Coppi, S. Migliuolo and F. Porcelli, Phys. Fluids, 31, 1630 (1988).

[13] F. Pegoraro, F. Porcelli and T.J. Schep, Phys. Fluids B1, 364 (1989).

[14] F. Pegoraro, T.J. Schep, Plasma Phys. Controlled Fusion 28, 647 (1986).

[15] A preliminary analysis of this modification is given in Section V of Ref. 7, where, however, the effect of resistivity is disregarded.

[16] H.L. Berk and Y.Z. Zhang, private communication.

[17] B. Coppi, R. Galvão, R. Pellat, M.N. Rosenbluth and P. Rutherford, Fiz. Plazmy 6, 961 (1976) [Sov. J. Plasma Phys. 2, 533 (1976)].

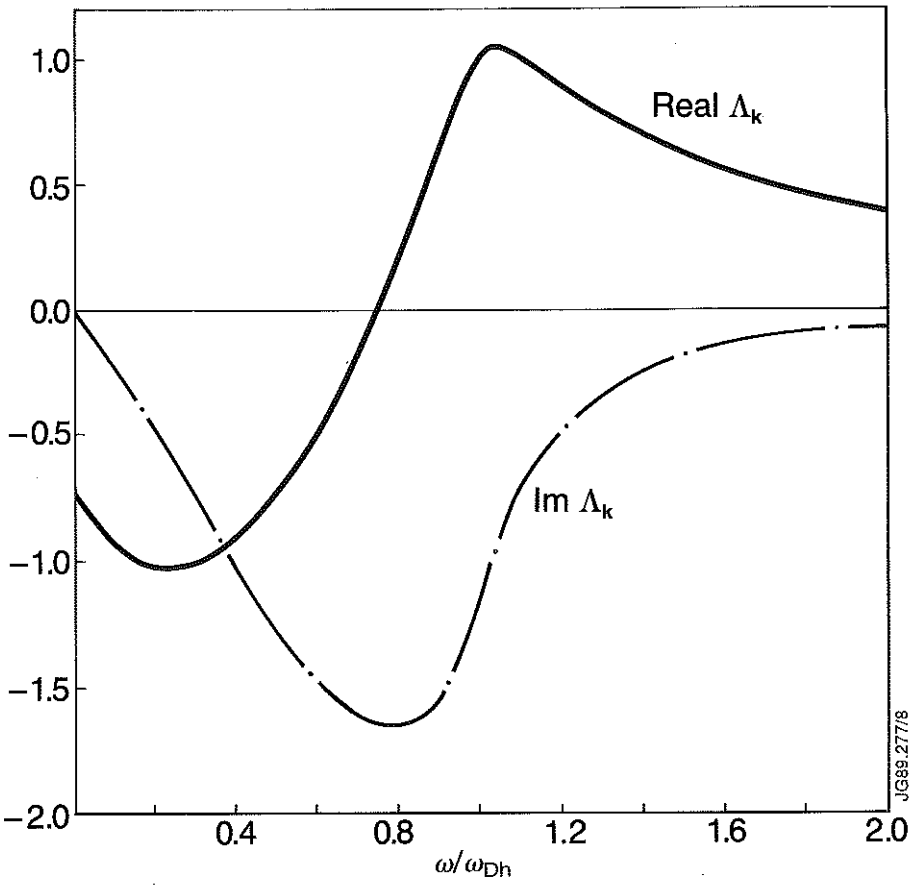

Fig.1 Real and imaginary parts of $\Lambda_K(\omega/\omega_{Dh}) \equiv (s_0/\beta_{ph}\varepsilon_0^{3/2})$ $\lambda_K(\omega/\omega_{Dh})$ for an isotropic slowing down distribution of energetic particles (from Ref. 7)

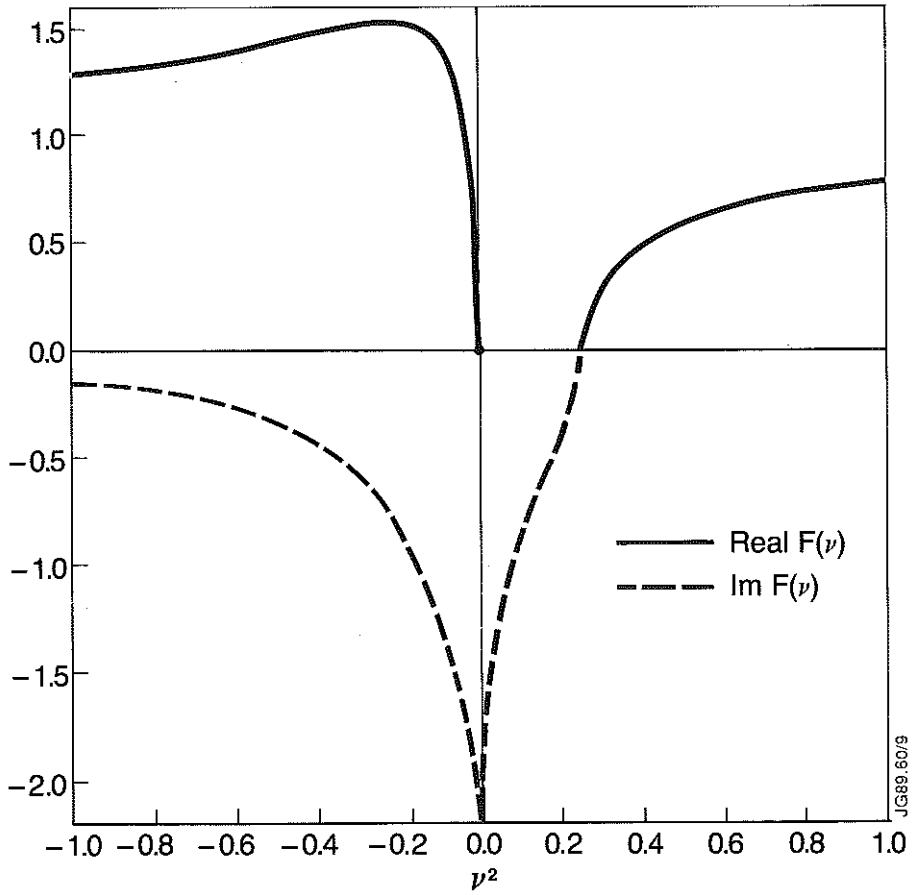

Fig.2 Real and imaginary parts of the function F(ν), defined in Eq.(6), versus real ν^2, defined in Eq.(7).

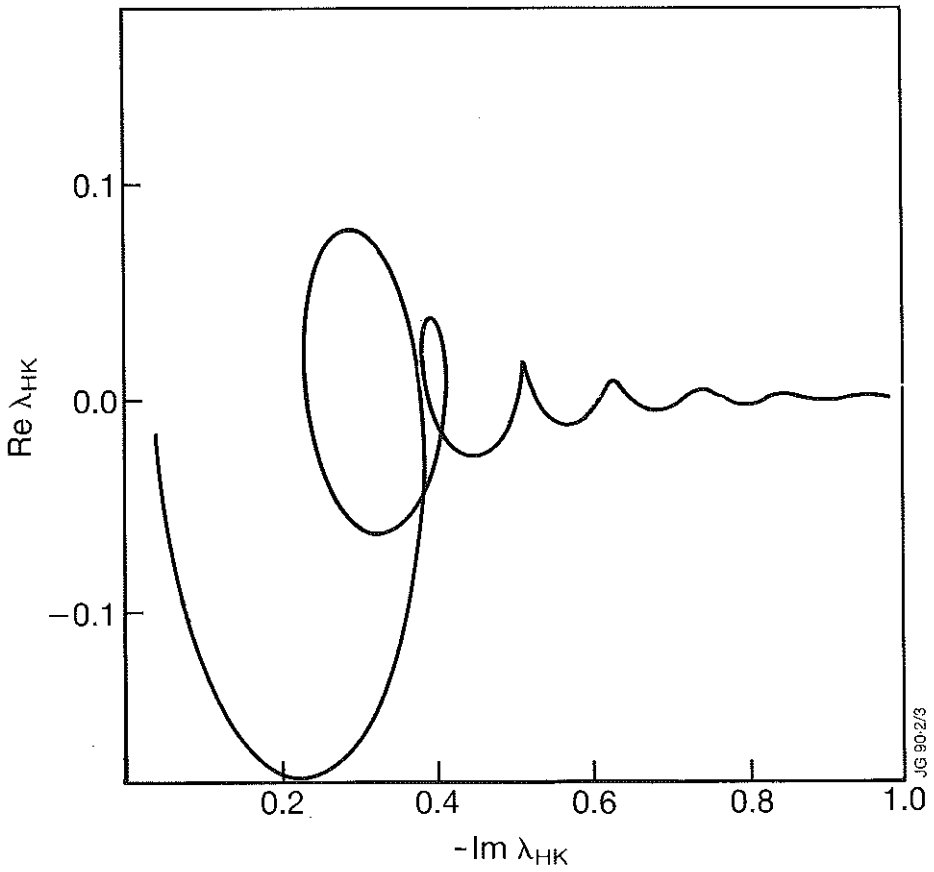

Fig.3 Re λ_{HK} versus Im λ_{HK} along the marginal stability curve for the following parameter values: $\omega_{di} / \omega_{Dh} = 0.7$; $\omega_\rho / \omega_{Dh} = 0.12$ and $\omega_\rho / \left(\omega_A \varepsilon_\eta^{1/3}\right) = 8.5$ corresponding to $\varepsilon\left(\omega_\rho\right) \equiv 1.5 \times 10^{-4}$.

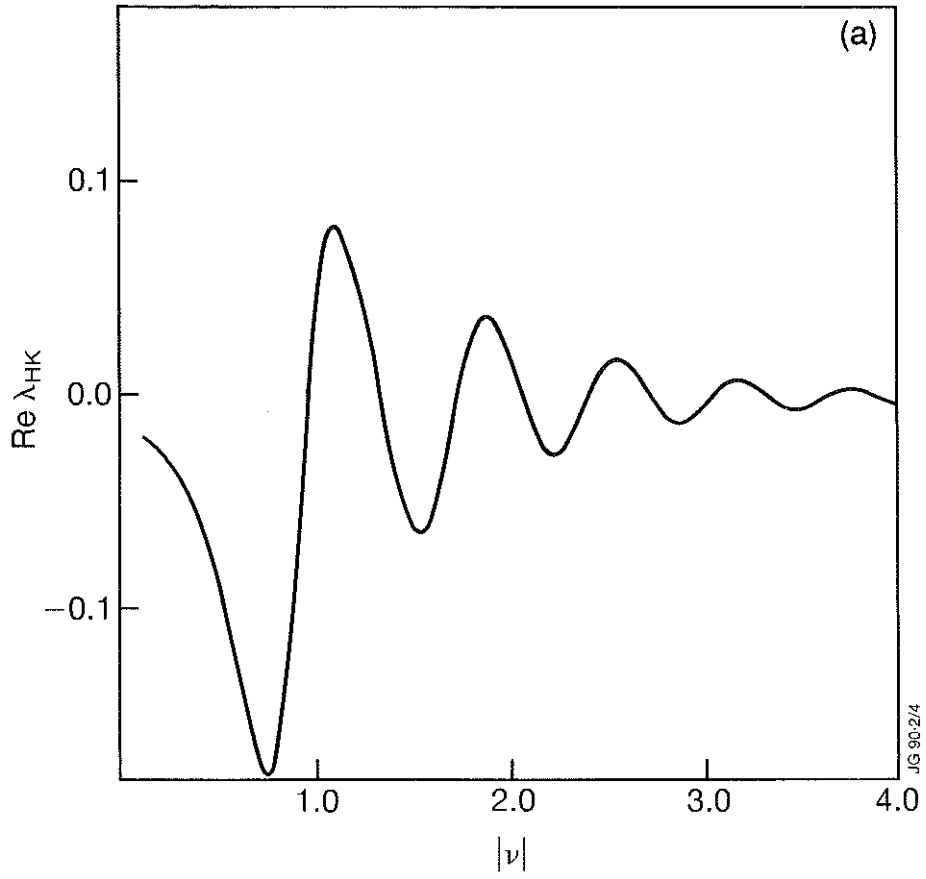

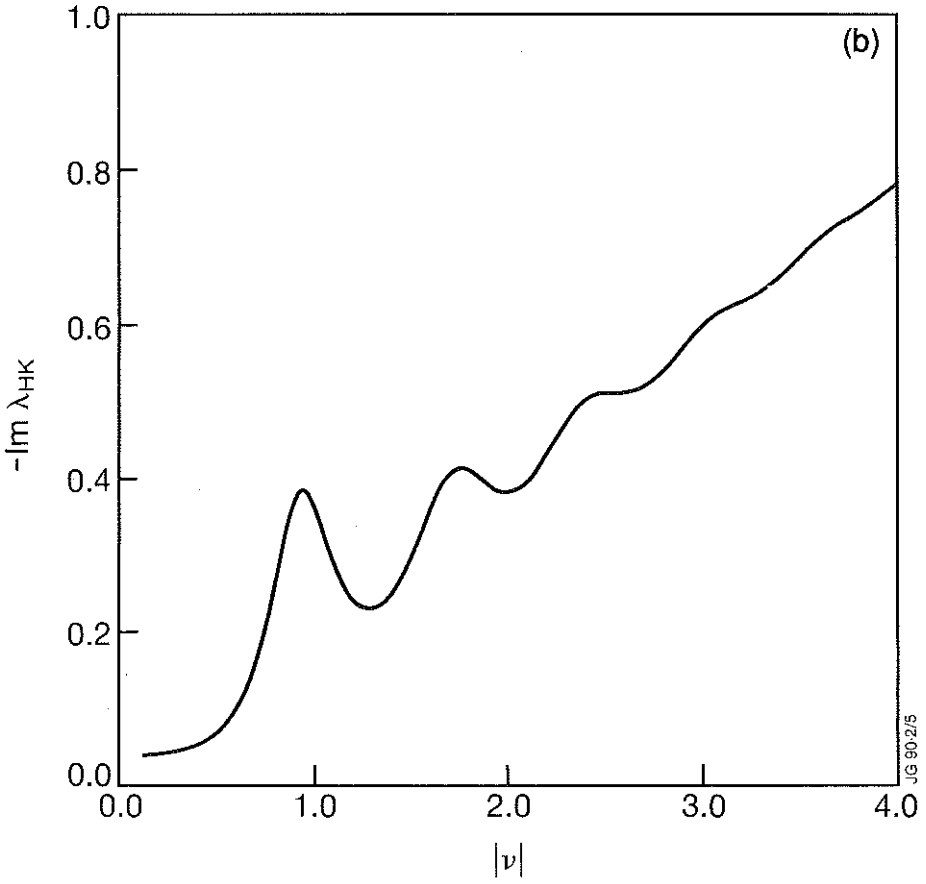

Fig. 4 Re λ_{HK} (a) and Im λ_{HK} (b) versus ν for ν^2 real and negative, and same parameter values as in Fig. 3.

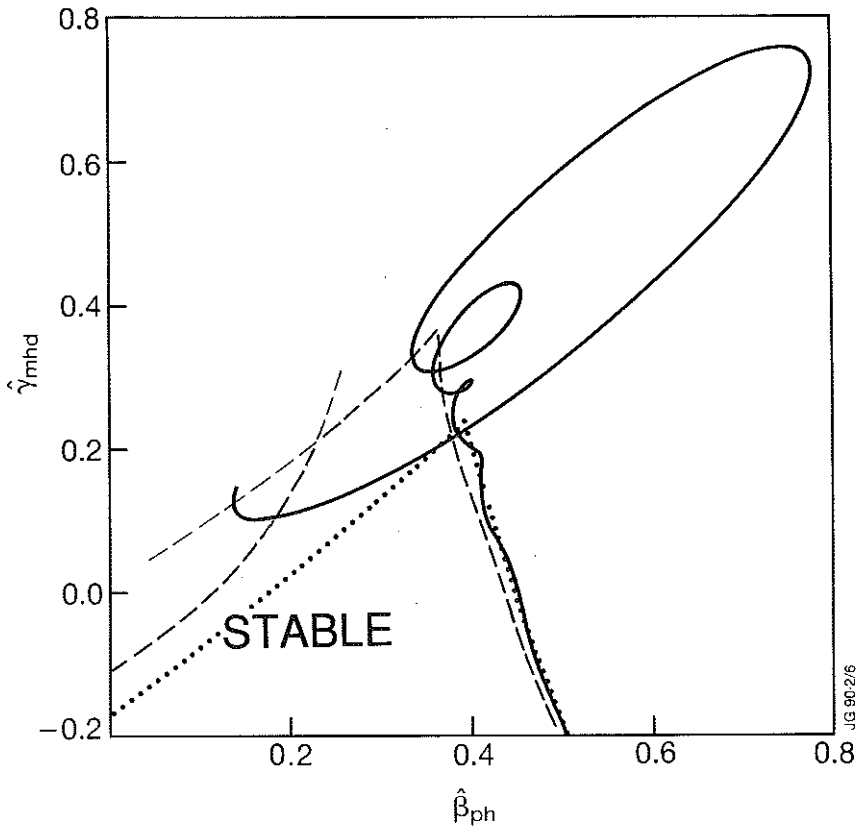

Fig. 5 Marginal stability curves in the $\left(\hat{\gamma}_{mhd}, \hat{\beta}_{ph}\right)$ plane. The solid line corresponds to marginal stability from the dispersion relation (4) for Re $\omega > \omega_{di}$. The stable domain lies below and to the left of this line Parameter values are the same as in Fig.3. The dotted curve corresponds to marginal stability from Eq.(11) for $\omega_\rho / \omega_{Dh} = 0.12$, $\varepsilon_\eta \equiv 0$ and growth rate $\gamma / \omega_\rho \to 0$. The dashed curves corresponds to the fluid core - ion limit of Ref.[4], with $\omega_{di} / \omega_{Dh} = 0.7$.

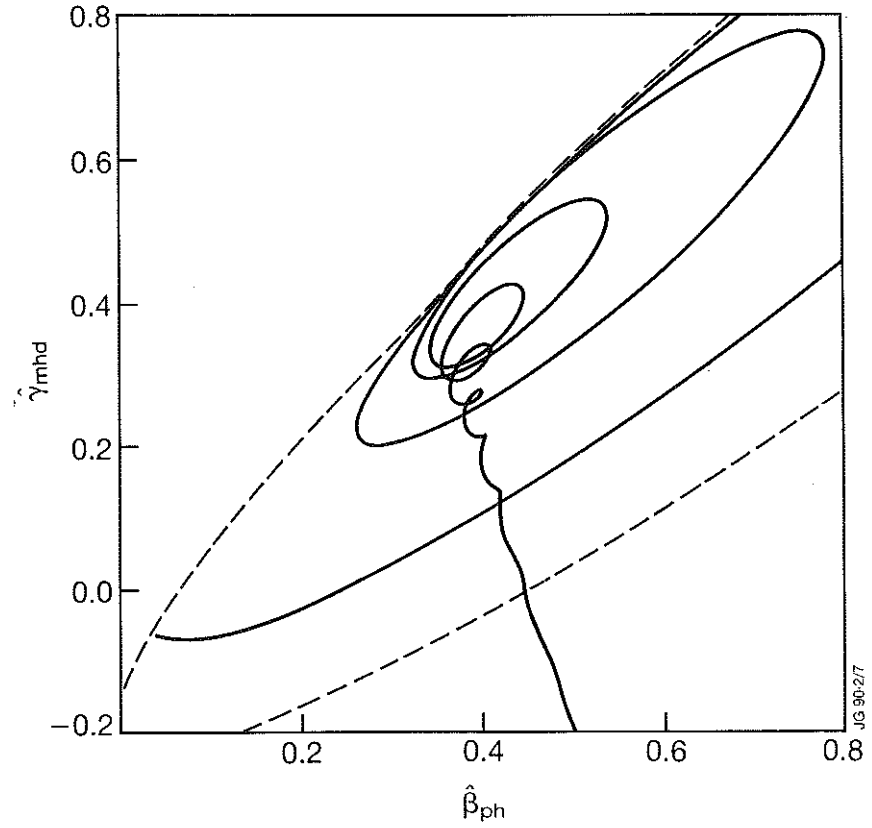

Fig. 6 Solid line: marginal stability curve for $\omega_{di} / \omega_{Dh} = 0.07$, $\omega_\rho / \omega_{Dh} = 0.12$, $\gamma / \omega_\rho = 10^{-3}$ and $\omega_\rho / \left(\omega_A \varepsilon_\eta^{1/3}\right) = 85$, corresponding to $\varepsilon\left(\omega_\rho\right) \equiv 1.5 \times 10^{-7}$. Many roots with Re $\omega \approx \omega_\rho$ are unstable within the spiral structure. In the limit $(\ell n 1/\varepsilon) \to \infty$, $\gamma / \omega_\rho \to 0$, taken in that order, the region occupied by the spiral structure tends to a limit area indicated by the dashed curve.